IEEE/CSC & ESAS European Superconductivity News Forum (ESNF), No. 6, October 2008
(ASC Preprint 5MX07 conforming to IEEE Policy on Electronic Dissemination, Section 8.1.9)

The published version of this manuscript appeared in *IEEE Transactions on Applied Superconductivity* **19**, No. 3, Part 2, 3403-3406, (2009)

The YBCO films with Zr^{4+} doping grown by MOD method

M. Liu, H. L. Suo, S. Ye, D. Q. Shi, Y. Zhao, L. Ma and M. L. Zhou

***Abstract*—$YBa_2Cu_3O_{7-\delta}$ (YBCO) films with Zr doping have been prepared successfully by the trifluoroacetate metal-organic deposition (TFA-MOD) method through dissolving Zr acetylacetonate into the precursor solution. Yttria-stabilized zirconia（YSZ）nanoparticles were detected in the doped YBCO films by XRD and SEM. From the analysis of XRD ω and φ scans, the doped films have better out-of-plane and in-plane textures than those of the un-doped YBCO film. Although the doped YBCO films have lower T_c than that of the un-doped YBCO film, a very significant enhancement of J_c is displayed as compared to the undoped film at applied fields. A high J_c near 10^5 A cm^{-2} at 2 T, 77K was observed in the Zr doped film, which is 30 times of the J_c values for the un-doped film in the same applied fields, indicating that an effective pinning force was created by Zr doping.**

***Index Terms*—Nanoparticle doping, TFA-MOD, YBCO film**

I. INTRODUCTION

For practical applications, especially power applications, high temperature superconductors (HTS) such as $YBa_2Cu_3O_{7-\delta}$ (YBCO) need to carry a high critical current density (J_c) under high magnetic fields. However, due to vortex motion, the capability of YBCO to carry currents is significantly reduced at higher applied magnetic fields. There is an effective way to improve the in-field performance of coated conductor by introducing various kinds of pinning centers using a variety of techniques, including interlayers of non-superconducting materials [1]−[2], mixed rare-earth doping [3][4], and doping with self-aligned $BaZrO_3$ (BZO) nanodots and nanorods [5]−[7], as well as the use of nanoparticle-modified substrate surfaces [8]−[9]. Among these approaches, BZO nanoparticles [7] [9] grown heteroepitaxially within laser-ablated YBCO films are the most popular, because these particles are easily incorporated into the films from a source target composed of a ceramic BZO/YBCO mixture. Using a pulsed laser deposition (PLD) process, Goyal [7] et al. have succeeded in producing long, nearly continuous vortex pins along the *c*-axis in YBCO, in the form of self-assembled stacks of BZO nanodots and nanorods, which led to an improvement in J_c in magnetic fields. Recently, a new strategy for introducing BZO nanoparticles into YBCO films has also been developed by J. Gutierrez et al. [10][11] on the basis of easily scalable chemical solution deposition techniques. The random crystalline orientation is the essential feature distinguishing chemically prepared nanocomposite films from those prepared through vacuum deposition methods. The quasi-isotropic character of the pinning has demonstrated that this new strategy is very effective in preventing vortex motion at high fields and high temperatures for all magnetic-field orientations. In this work, epitaxial YBCO/YSZ nanocomposite thin films were grown from a non-vacuum, low cost, and easily scalable metal–organic deposition method, and their microstructures and physical properties were investigated.

Manuscript received August 20, 2008. This work was supported by the National Basic Research Program 973 of China (2006CB601005), National Natural Science Foundation of China (50771003), National High Technology Research and Development Program of 863 (2007AA03Z242)and the program of a Foundation for the Author of National Excellent Doctoral Dissertation of China (200331).

M. Liu, H. L. Suo, S. Ye, Y. Zhao, L. Ma and M. L. Zhou are now with College of Materials Science and Engineering, Beijing University of Technology, Beijing, 100022 China. (corresponding author: M. Liu; phone: +86-010-673-929-47; fax: +86-010-673-929-47; e-mail:Lm@bjut.edu.cn)

D.Q. Shi is now with the Institute for Superconducting and Electronic Materials, the University of Wollongong, NSW 2522 , Australia (e-mail: dongqi@uow.edu.au).

II. EXPERIMENTAL

The trifluoroacetate precursor solution was prepared by a standard TFA-MOD process with a cation ratio of Y: Ba: Cu=1: 1.5: 3. A Zr acetylacetonate precursor in stoichiometric proportions was added to obtain the TFA precursor solution with 6 mol. % Zr doping. The solution was coated on 10 × 10 mm^2 $LaAlO_3$ single-crystal substrates with (001)-orientation by spin coating at a speed of 4000 rpm for 2 min at room temperature. The wet films were decomposed to amorphous precursor films by slowly heating them up to 400°C in a humid oxygen atmosphere. The amorphous precursor film was heated up to 800°C in humid Ar/O_2 (100 ppm O_2) atmosphere and held for 90 minutes. An oxygenation process was carried out at 550−450°C for 90 min to achieve the superconducting phase.

X-ray diffraction measurements were carried out to examine the phase of the YBCO films. X-ray ω-scans and φ-scans were used to evaluate the out-of-plane and in-plane textures of the YBCO films, respectively. The surface morphology of the films was examined with scanning electron microscopy (SEM). The film thickness after growth was determined, by profilometer analysis, to be 250−300 nm. The DC magnetization measurements were carried out with a physical properties measurement system (PPMS) in magnetic fields parallel to the *c*-axis of the specimens. The J_c values of the YBCO films in magnetic fields were determined by application of the Bean critical state model formula, $J_c(H) = 20\triangle M(H)/a(1-(a/3b))$, where $\triangle M$ is the vertical width of the magnetization hysteresis loop (emu cm^{-3}), and a and b (cm) are the cross-sectional dimensions of the sample perpendicular to the applied field, with $b \geq a$.

III. Results And Discussion

A. Phases

Figure 1a shows X-ray diffraction patterns of the un-doped and doped YBCO films. Only (00l) diffraction peaks of YBCO were observed, which indicates a well-textured, *c*-axis oriented grain structure. In order to obtain further information on phases, XRD of the samples was conducted at a very low scan speed. As shown in Figure 1b, $Cu_2Y_2O_5$ impurity was detected in both un-doped and doped YBCO films because of the use of a Barium-poor starting solution, which is consistent with the literature [12] [13]. K. Nakaoka et al investigated the influence of the starting solution compositions with different molar ratios of Y:Ba:Cu = 1.0:1.0–3.0:3.0 on both the microstructure and superconducting properties of YBCO films by the advanced TFA-MOD process. They found that highest J_c value was obtained not at a Ba/Y molar stoichiometric proportion of 2.0, but at a Ba/Y molar ratio of 1.4–1.6 owing to the size and the number of pores decreasing. Furthermore, CuO and $Cu_2Y_2O_5$ nanoparticles were also recognized in the YBCO films fabricated by using the Ba-poor starting solutions. They explained these nano-particles of CuO and $Cu_2Y_2O_5$ in the YBCO grains may act as pinning centers to improve the dependence of I_c values on magnetic field angle. So, we chose a Ba/Y molar ratio of 1.5 in both pure and Zr $^{4+}$ doping YBCO coating solution.

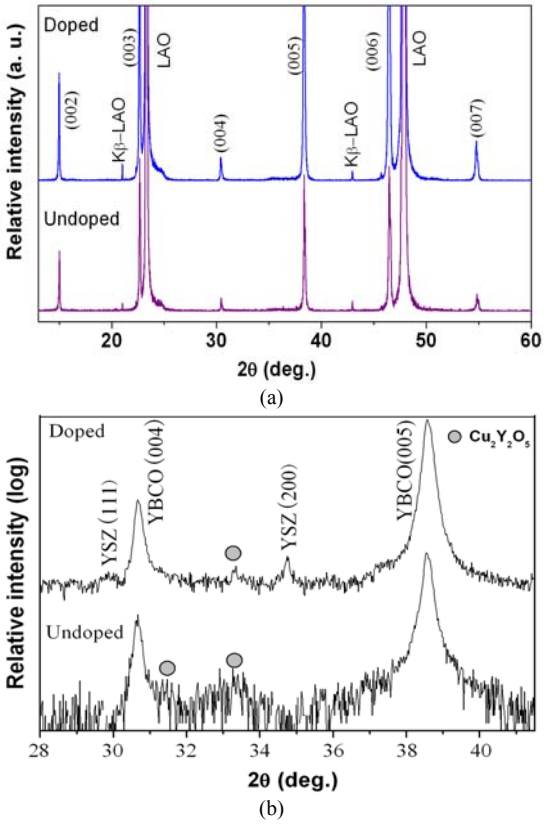

Fig. 1. (a) X-ray diffraction patterns of undoped YBCO film and YBCO films with different doping levels of Zirconium. (b) Enlargement of a section of (a) showing the presence of $Cu_2Y_2O_5$ impurity.

We found that Yttria-stabilized Zirconia (YSZ) phase was detected in the YBCO films with Zirconium doping, which is not consistent with other reports [13][14]. $BaZrO_3$ phase was identified in the YBCO films with Zr doping fabricated by Gutierrez J. [13], which is formed via a reaction each other of the decomposition compound of Zr and Ba precursor salts. However, due to the use of Barium-poor solution in our experiment, the decomposition compounds of Zr precursor salt are easier to react with the decomposition compounds of excess Y salt to form YSZ phase. Furthermore, according to the x-ray patterns, the intensity of the YSZ (111) peak is lower than that of the (200) peak, while the theoretical value of the YSZ (111) peak is much higher than that of the (200) peak, indicating the coexistence of epitaxial and randomly oriented YSZ nanodots. From the full-width at half-maximum (FWHM) of the YSZ (200) and (111) peaks and the Scherrer formula (Dc = 0.89λ / (B cos θ), where Dc is the size of the YSZ particle. λ is 0.15406 nm, which is the wavelength of the characteristic X-ray from a Cu target. B and θ are the full-width at half-maximum and the diffraction angle of theYSZ (002) and (110) peaks, respectively.) We estimated that the size of the YSZ nanodots was in the range of 10−20 nm. Their dimensions are of the order of the coherence length of YBCO, and so they can act as flux pinning centers.

B. Texture

X-ray diffraction ω and φ scans were collected to determine the out-of-plane and in-plane alignments of the films, respectively. It can be clearly seen from Fig. 2 that the FWHM values of the ω and φ scans for the doped YBCO films are 0.35^o and 1.07^o, respectively, which are smaller than those of the un-doped YBCO film, indicating that the doped films have better biaxial textures.

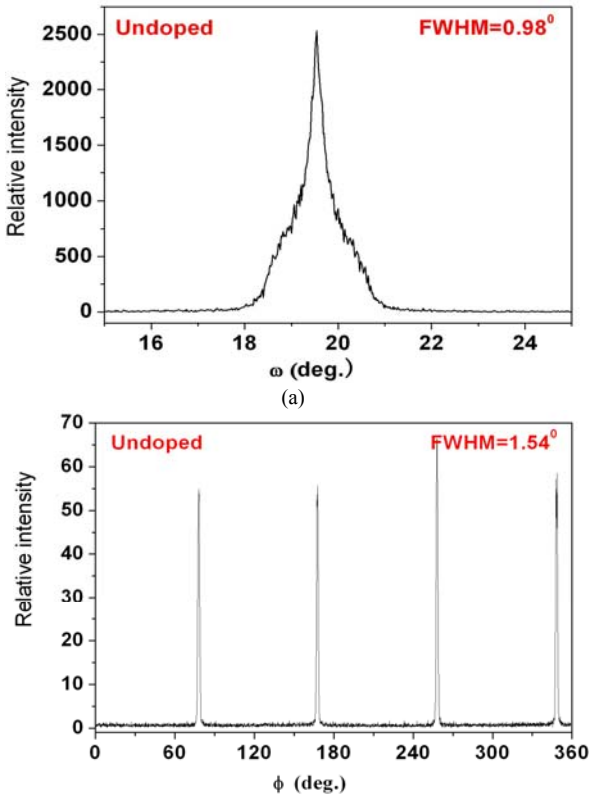

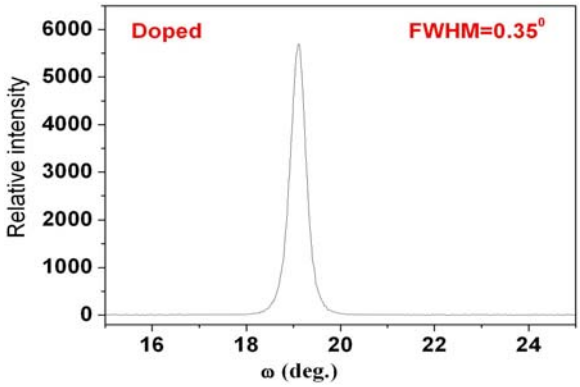

(c)

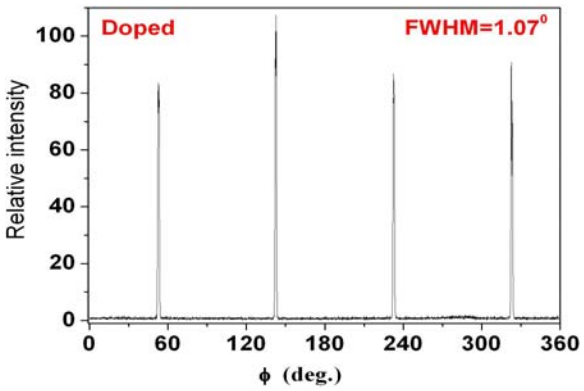

(d)

Fig. 2. FWHM values of the ω scan (a) and φ scan (b) for undoped YBCO films; FWHM values of the ω scan (c) and φ scan (d) for doped YBCO films.

C. *Surface Morphology*

Figure 3 shows the SEM surface morphologies of undoped and doped YBCO films. Compared with the pure YBCO film, the Zr-doped YBCO film has a denser and smoother surface, and the grains are grown as large interconnected platelets that lie parallel to the surface, which will lead to a strong biaxial texture of the doped YBCO films. Additionally, as shown in the inset of figure 3(b), many nanosized particles (marked by arrows) are uniformly distributed in the doped YBCO film while no such particle was found in the un-doped YBCO film. The size of these particles is around 20nm so that the common EDS we used can not accurately analyze their composition. We guess that they should be YSZ nano-crystals combining with their size and the results of XRD.

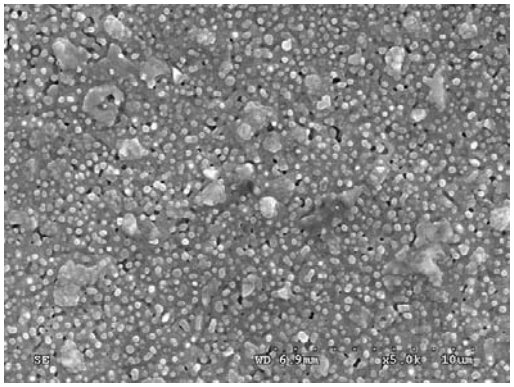

(a)

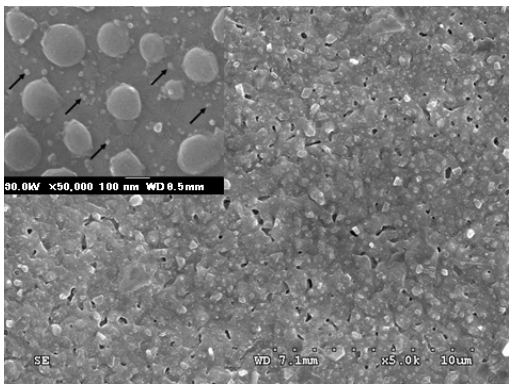

(b)

Figure 3. SEM surface morphologies of the pure YBCO film (a) and a typical doped YBCO film (b). (The inset in figure 3(b) is a larger magnification image showing the presence of nanosized particles in the doped film.)

D. T_c

The critical temperature of samples was measured via a physical properties measurement system. As shown in figure 4, both un-doped and doped films have the same transition width. However, the $T_{c,\ onset}$ of the doped YBCO film is 1.5K lower than that of the un-doped film. The lowering of T_c in the presence of the nanoparticles is consistent with other studies done on PLD YBCO films that were doped with Y_2O_3 nanoparticles [14]. The reason for the depressed T_c may possibly be Zr diffusion into the YBCO, which might result in Zr substitutions into Yttrium sites, which are able to locally depress T_c.

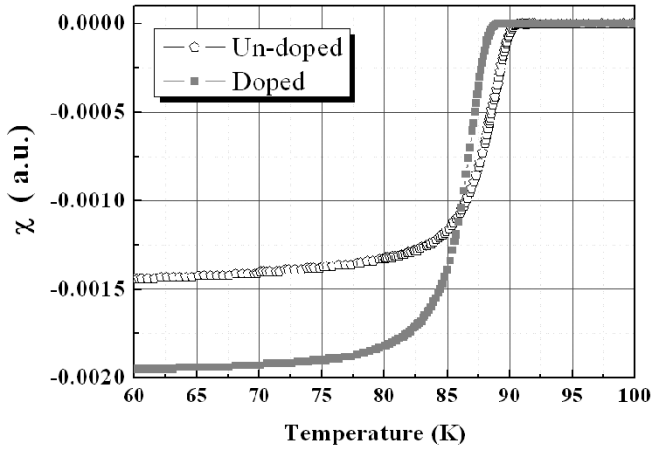

Fig. 4. The T_c of both doped and un-doped YBCO films.

E. J_c

Devices with YBCO films are usually used at a temperature of 77 K, so we measured the J_c at 77 K using PPMS. Figure 5 shows the field dependence of J_c at 77 K, with the field parallel to the *c*-axis. It can be seen that the 6% Zr doped film has a very significant enhancement of J_c values as compared to the un-doped film for all applied fields. A high J_c near 10^5 A cm^{-2} at 2 T was obtained in the 6% doped Zr film, which is 30 times of J_c value for the un-doped film in the same applied fields, indicating that an effective pinning force was created by 6% Zr doping. The overall increase in J_c at all magnetic fields can be more clearly seen when the magnetic-field dependence of the pinning force, $F_p = J_c(B) \times B$, is presented, as shown in Fig.

5(b). Although J_c decreases monotonically with increasing field, F_p increases to a maximum value $F_{p,max}$ at the field of 0.3 T field, then slowly decreases during further increase of the applied field. $F_{p,max}$ of 3.0 GNm^{-3} in the 6% Zr doped YBCO film, which is a close to 500% enhancement compared with that of the un-doped sample, clearly exemplifies the appealing prospects for the present nanocomposite films.

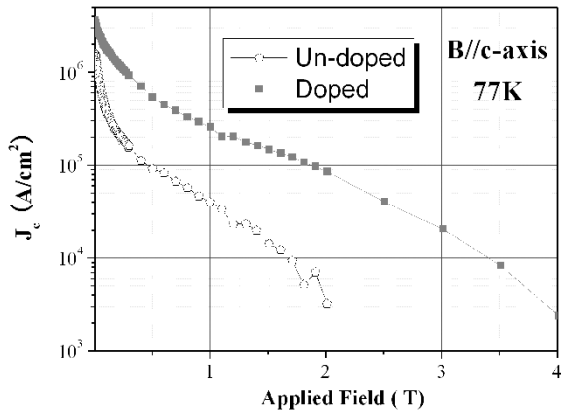

(a)

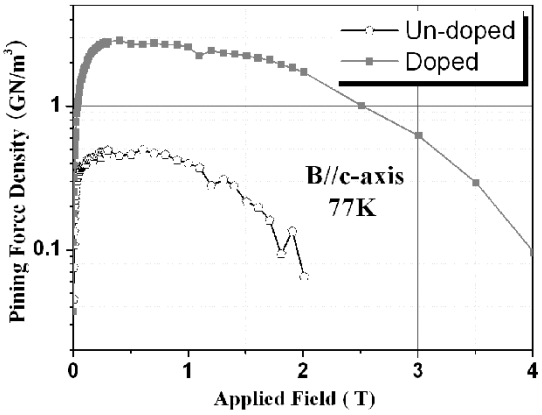

(b)

Fig. 5. The field dependence of J_c (a) and the pinning force (b) at 77 K, with the field parallel to the *c*-axis.

IV. Conclusion

In conclusion, we have shown that the metal-organic deposition technique can be modified to be used as a cost-effective and highly versatile method for introducing nanosized pinning centers into YBCO films. The TFA-YBCO route with Zr doped precursor solutions was utilized to fabricate YSZ doped YBCO films through an *in-situ* crystallization process. Investigations into the behavior of the critical current density in magnetic fields reveal a strong enhancement of J_c at high magnetic fields in the YBCO film with 6% Zr doping. Pinning centers introduced by chemical solution deposition techniques show enhanced pinning properties in all magnetic fields.

Acknowledgment

The authors would like to thank Prof. S. X. Dou (University of Wollongong) for his valuable suggestions in preparing this paper.

References

[1] Q. X. Jia, S. R. Foltyn, P. N. Arendt, and J. F. Smith, **"**High-temperature superconducting thick films with enhanced supercurrent carrying capability," ***Appl. Phys. Lett.***, vol. 80, no. 9, pp. 1601-1603, Mar. 2002.

[2] S. R. Foltyn, H. Wang, Q. X. Jia and P. N. Arendt**, "**Overcoming the barrier to 1000 A/cm width superconducting coatings, " *Appl. Phys. Lett.,* vol. 87, no. 16, pp. 162505-1-162505-3, Oct. 2005.

[3] J. L. MacManus-Driscoll, S. R. Foltyn, Q. X. Jia, H. Wang, A. Serquis, B. Maiorov, L. Civale, Y. Lin, M. E. Hawley, M. P. Maley, and D. E. Peterson*, "*Systematic enhancement of in-field critical current density with rare-earth ion size variance in superconducting rare-earth barium cuprate films*," Appl. Phys. Lett.,* vol. 84, no. 26, pp. 5329-5331, Jun. 2004.

[4] C. Cai, B. Holzapfel, J. Hänisch, L. Fernandez and L. Schultz, "High critical current density and its field dependence in mixed rare earth (Nd,Eu,Gd)$Ba_2Cu_3O_{7-\delta}$ thin films, " *Appl. Phys. Lett.,* vol. 84, no. 3, pp. 377, Jan. 2004.

[5] S. Kang, A. Goyal, J. Li, A. A. Gapud, P. M. Martin, L. Heatherly, J. R. Thompson, D. K. Christen, F. A. List, M. Paranthaman, and D. F. Lee, "High-Performance High-T_c Superconducting Wires, " *Science ,* vol. 311, no. 5769, pp. 1911-1914, Mar. 2006.

[6] Y. Yamada, K. Takahashi, H. Kobayashi, M. Konishi, T. Watanabe, A. Ibi, T. Muroga, S. Miyata, T. Kato, T. Hirayama, and Y. Shiohara, **"**Epitaxial nanostructure and defects effective for pinning in Y(RE)$Ba_2Cu_3O_{7-x}$ coated conductors, "*Appl. Phys. Lett.,* vol. 87, no. 13, pp. 132502-1-132502-3, Sept. 2005.

[7] A. Goyal, S. Kang, K. J. Leonard, P. M. Martin, A. A. Gapud, M. Varela, M. Paranthaman, A. O. Ijaduola, E. D. Specht, J. R. Thompson, D. K. Christen, S. J. Pennycook and F. A. List, "Irradiation-free, columnar defects comprised of self-assembled nanodots and nanorods resulting in strongly enhanced flux-pinning in YBa2Cu3O7-δ films, " *Supercond. Sci. Technol.,* vol. 18, no. 11. pp. 1533-1538, Nov. 2005.

[8] A. Crisan, S. Fujiwara, J. C. Nie, A. Sundaresan and H. Ihara, **"**Sputtered nanodots: A costless method for inducing effective pinning centers in superconducting thin films,**"** *Appl. Phys. Lett. ,* vol. 79, no. 27, pp. 4547-4549, Dec. 2001.

[9] J. L. MacManus-Driscoll, S. R. Foltyn, Q. X. Jia, H. Wang, A. Serquis, L. Civale, B. Maiorov, M. E. Hawley, M. P. Maley and D. E. Peterson, "Strongly enhanced current densities in Superconducting coated conductors of YBa2Cu3O7–x + BaZrO3," Nat. Mater. , vol. 3, no. 7, pp. 439-443, Jul. 2004.

[10] J. Gutierrez, A. Llordes, J. Gazques, M. Gibert, N. Roma, S. Ricart A. Pomar, F. Sandiumenge, N. Mestres, T. Puig and X. Obradors, "Strong isotropic flux pinning in solution-derived $YBa_2Cu_3O_{7-x}$ nanocomposite superconductor films," 2007 *Nature Materials,* vol. 6, no. 5, pp. 367-373, May. 2007.

[11] Y. X. Zhou, S. Ghalsasi, I. Rusakova and K. Salama, "Flux pinning in MOD YBCO films by chemical doping," *Supercond. Sci. Technol.,* vol. 20, no. 9. pp. S147-S154, Sept. 2007.

[12] K. Nakaoka, J. Matsuda, Y. Kitoh, T. Goto, Y. Yamada, T. Izumi and Y. Shiohara, "Influence of starting solution composition on superconducting properties of YBCO coated conductors by advanced TFA-MOD process, " *Physica C,* vol. 463-465, pp. 519-522, May. 2007.

[13] J. Matsuda, K. Nakaoka, T. Izumi, Y. Yamada and Y. Shiohara, "Effect of Ba/Y ratio in starting solution on microstructure evolution of YBCO films deposited by advanced TFA-MOD process, " *Physica C,* vol. 468, pp. 997-1005, May. 2008.

[14] P. Mele, K. Matsumoto, T. Horide, A. Ichinose, M. Mukaida, Y. Yoshida and S. Horii, "Insertion of nanoparticulate artificial pinning centres in $YBa_2Cu_3O_{7-x}$ films by laser ablation of a Y_2O_3-surface modified target, " ***Supercond. Sci.*** *Technol*., vol. 20, no. 7. pp. 616-620, Jul. 2007.